A quadratic programming approach for the mosaicing of virtual slides that incorporates the positioning accuracy of the microscope stage

Dirk Steckhan*
Image Processing and Medical Engineering Department
Fraunhofer-Institute for Integrated Circuits IIS
91058 Erlangen, Germany
dirk.steckhan@iis.fraunhofer.de

Dietrich Paulus**
Arbeitsgruppe Aktives Sehen
Institute for Computational Visualistics
University of Koblenz-Landau
56016 Koblenz, Germany
paulus@uni-koblenz.de

***Abstract*— We describe a novel approach for creating virtual slides that incorporates the positioning accuracy of the microscope stage in the optimization step. To capture a complete slide in microscopy, a large number of fields of view have to be acquired by moving the microscope stage in a controlled way. These fields of view are aligned in such a way that a globally consistent virtual slide is formed. However, depending on the positioning repeatability of the stage and the accuracy of the stage calibration, this results in alignment errors. These errors are usually resolved by applying a mosaicing algorithm. Our algorithm extends known mosaicing approaches by analyzing the positioning accuracy of the stage and incorporating this knowledge to make the mosaicing process more robust.**

I. Introduction

Conventional light microscopy is one of the most commonly used and most powerful techniques for the inspection and diagnosis of biological probes. However it is constrained by several factors. Stain colors can change or fade with time. This is particularly true for immunofluorescence staining techniques that are often only useful in a very small time frame[1]. Biological Probes tend to age. Slides are unique and cannot be reproduced for example the slide glass can easily break [1], [2]. Microscopes only visualize a small part of a slide at a time and magnifications are limited to the available objectives. Simultaneous viewing is constrained to a very small group of observers and the slide has to be physically present. It is not possible to annotate regions of interest on the slide.

One goal of virtual microscopy is to solve these problems by replacing the direct work with the microscope and the slide with the use of digitized probes. For this purpose the slide is scanned once by a fully automatized robotic microscope and saved digitally. Such a digitized probe has none of the problems mentioned above. Additionally it even can be examined from afar on any computer as if it was physically present. Areas of interest, for example cancerous cells, can be annotated on the slide and thus, it is still possible to retrace why an examiner made a specific diagnosis later on. Thus, in the long run virtual microscopy can potentially replace traditional microscopy.

Nevertheless, there are still impediments that have not been entirely solved. This article covers one of these impediments: the correct alignment of all fields of view (FoV) in biological probes with large areas of no information content, such as probes from cytometry. A slide is simply too large to be captured with one image at a reasonable magnification. Considering the case of 20-fold magnification and a typical color camera, that produces a $1000 * 1000$ pixel image and has a cell size of $7.4\mu\mathrm{m} * 7.4\mu\mathrm{m}$. This means, that each pixel covers an area of $0.37\mu\mathrm{m} * 0.37\mu\mathrm{m}$ and each field of view captured an area of $0.37\mathrm{mm} * 0.37\mathrm{mm}$. Of course it depends on the kind of probe scanned, however to give an example, if the valid area that has to be scanned is $2\mathrm{cm} * 3\mathrm{cm}$, this means that roughly $55 * 82 = 4510$ FoV have to be acquired. The scanning process of the slide to be virtualized is usually done by computer-controlled motorized stages, which must furthermore be accurately calibrated. However, no matter how carefully calibrated, motorized stages have positioning errors that are bound to accumulate during the scanning process, and therefore lead to alignment errors in the virtual slide. Thus, one major challenge in virtual microscopy is the development of algorithms that align all acquired FoV in such a way that the originally scanned slide is completely reconstructed.

The conventional approach for the mosaicing is to scan the slide in a first step and in a second step to register each FoV with its neighboring FoV, followed sometimes by an optimization stage. The schematic Fig. 1 shows the difference between a mosaic obtained by optimization and one that has been acquired by naive consecutive alignment.

The necessity of the optimization scheme is obvious if one considers three images that have been registered to each other and thus result in three transforms. In a perfect environment these transforms will result in an overdetermined but consistent system of equations; when concatenated they result in an identity transform. However since the transforms are measurements on real-world images that are subject to noise and other degradations, they are prone to error. The idea of optimization is then to minimize the average measurement errors by distributing them for example equally over all transforms or, if a measurement of the reliability of the

*D. Steckhan is a research associate at the Fraunhofer-Institute for Integrated Circuits IIS. Additionally, he is a PhD student at the University of Koblenz-Landau and the International Max-Planck Research School for Optics and Imaging, 91058 Erlangen, Germany

**D. Paulus is professor for *Computervisualistik* (Computational Visualistics) at Koblenz-Landau University, Koblenz, Germany

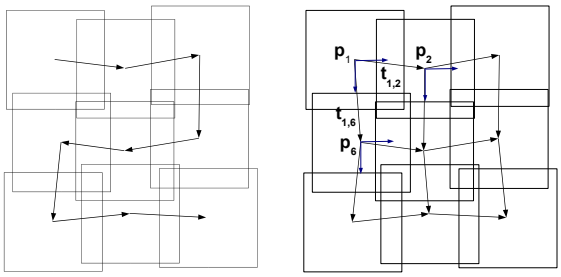

(a) (b)

Fig. 1. In (a) a schematic of a consecutive alignment process is depicted. In consecutive alignment only the transform parameters from the direct predecessor is taken into account. In a global optimization scheme all transform parameters from the adjoining images are taken into account as depicted in (b). Additionally in (b) three images are marked with their image coordinate systems and their global positioning $\mathbf{p}_i$. The two translational vectors $\mathbf{t}_{i,j}$ that casts those images in the coordinate space of each other are also marked.

transforms is given, giving more reliable transforms a higher priority.

In this paper we focus on the optimization step. Usually the optimization step is completely detached from the image acquisition step. However, if one analyzes the positioning accuracy of the stage, it is clear that the positioning varies in a specific area. We utilize this knowledge to make the optimization step more robust by specifying upper and lower bounds for the possible image repositioning in the mosaicing process. The problem of optimization is solved using quadratic programming with inequality constraints.

We outline related work in Sec. II. Image acquisition is described in Sec. III. We present our approach to image mosaicing in Sec. IV and give an evaluation in Sec. V before we conclude in Sec. VI.

II. Related Works

Mosaicing algorithms usually can be divided into two separate steps. In the first step neighboring images are pairwise registered by applying area-based or feature-based registration algorithms. The transform parameters estimated are then in a second step bundle adjusted to retrieve a globally consistent transform space. *Szeliski* [3] has presented an authoritative survey of both local and global image stitching methods. Szeliski's focus however lies on multiple viewpoint image alignment and the generation of panoramas under affine transform constraints. This is a more general problem than the one in virtual microscopy, where the transform space of the images is strictly translational. Thus, this problem allows for more specialized mosaicing algorithms.

In his article on the stitching of scenes with moving objects, *Davis* [4] derived a system of linear equations from pairwise registrations and solved it using a least squares approach to get a globally optimized transform space. Problematic about Davis' approach is that by solving the system in a least square sense, he distributes the error equally over all transforms. This can only be justified if the error in the transforms is strictly Gaussian. *Kang et al.* [5] proposed a graph-theoretic approach for the global registration of 2D mosaics under projective transform constraints.

Surprisingly, only a few articles can be found in literature that deal with the stitching of virtual slides directly. *Sun et al.* use feature matching with the Harris-Corner Detector and they do a global geometric correction with an objective function that minimizes the Euclidean distance between the feature points when the transform is applied [6]. *Appleton et al.* approach the image stitching problem as a global optimization problem [7]. They use dynamic programming and a similarity function to place a complete row of images with respect to previously placed rows at a time. However, since they only place one row at a time this is only partly a global optimization which would require placing all images at once. Additionally they needed an overlap of 45% between images in order to get good results. This results in a very large scan time. In a previous paper [8] we utilized Davis' [4] idea of creating a system of linear equations for the optimization step and extended it by weighting each transform according to its reliability. Thus we could solve the equation system in a weighted least square sense. This approach gave objectively improved results compared to the unweighted solution. However under certain circumstances this approach still exhibits errors. Mostly on slides with significantly big areas of low information content and thus low correlation values some of the images in these areas are not correctly repositioned.

III. Image Acquisition

Within this work images were acquired using a fully automatized microscopy system consisting of a Leica DM6000B microscope with a z-axis, a motorized stage by Ludl Electronic Products and a color camera, model Pike by Allied Vision Technologies. For the examples of cervical cytometry and histology, images were acquired using a $20\times$ dry objective. The blood smear slides were scanned using a $10\times$ dry objective. The camera produces a $1000 * 1000$ pixel image with a CCD chip of $10.5\mathrm{mm}$ diagonal and an effective cell size of $7.4{*}7.4\mu\mathrm{m}$. $0.37{*}0.37\mu\mathrm{m}^2$ for the $20\times$ dry objective. The stage camera system was carefully calibrated in order to get an accurate transform between pixel coordinates of the camera and hardware coordinates of the stage. However with a resolution of $0.4\mu\mathrm{m}$, a repeatability of $2.0\mu\mathrm{m}$ and an accuracy of $10.0\mu\mathrm{m}$ for the stage used in our system, image alignment cannot be done just by accurately moving the stage.

The slides are scanned using a meandering strategy (alternating left to right, right to left and top to bottom). Acquisition of images was done with an overlap of 20% between adjacent images of the image size. Thus an estimate of where each image on the virtual slide is positioned and how they overlap is already known.

IV. Image Mosaicing

Image Mosaicing in virtual microscopy is the geometric reconstruction of the actual slide from many fields of view. Modern microscopy systems, as for example used in clinical

work areas and also in our setup, are already corrected with regard to most geometric distortions. Thus the dominant source of error is translational and the transform space can be restricted to two parameters, which are the translations in x- and y-direction. The goal of stitching is to align each field of view with the neighboring fields in such a way that there are almost no visible geometric distortions.

Our algorithm is divided into three steps. In the first step, the transformations between each field of view and its direct neighbors, and how well they match, is determined. In the second step, these parameters are used to get an estimate of the positioning accuracy of the stage. This knowledge is utilized to statistically specify upper and lower bounds for the possible relocation of the images. In the final step, a weighted equation system is formed using the transform parameters from the first step that is inequality constrained by the parameters from the second step. This system can be transformed to an inequality constrained quadratic programming problem. Such a system is solvable using the *Karush-Kuhn-Tucker* theorem.

A. Transform determination and equation system formulation

The determination of the transformations and the equation system has been presented in our previous work [8]. Here we will only give a short introduction for the sake of completeness.

As in our previous works [8] and [9] we choose the inversely transformed normalized cross power spectrum with *Foroosh et al's* [10] extension for subpixel accuracy for the determination of the transformation between two adjoining images. It can be shown that cross-correlation is the optimal statistical estimator function under the assumption of translational displacement and additive white Gaussian noise [11]. For the case of the normalized cross power spectrum this cannot be analytically shown. However, contrary to cross-correlation, the inversely transformed normalized cross power spectrum has the advantage that the correlation energy is completely concentrated in one point or in the case of subpixel displacement in the direct neighborhood of the peak. The ease and security of detecting this point makes the inversely transformed normalized cross power spectrum a very attractive method for image processing. Additionally this method gives a measurement of the quality of the determined transform. Two images that perfectly match and are not corrupted by any noise would give a correlation value of one as peak correlation value. Consequently lower correlation values are a hint that the resulting transforms are less reliable. Note, that in light microscopy the area with no information content is always white, since the light can pass unobstructed through the slide and the optics to the detector. This means, if one correlates two images taken at areas of the slide with no information content, this would result in a correlation value close to the maximum of one. To avoid this problem, we invert each image.

For each field of view (besides the right and bottom border images) the translation to its right, and to its bottom neighbor is determined as depicted in Fig. 1b. The global positioning $\mathbf{p}_j$ of image I_j can be calculated by first calculating the positioning of the neighboring image $\mathbf{p}_i$ of image I_i and using the translation vector $\mathbf{t}_{i,j}$ to cast image I_i in the space to image I_j:

$$\mathbf{p}_j = \mathbf{p}_i + \mathbf{t}_{i,j} \rightarrow \mathbf{p}_j - \mathbf{p}_i = \mathbf{t}_{i,j} \text{ with } 1 \leq i,j \leq N. \quad (1)$$

If the image I_1 is set to the origin of the virtual slide coordinate system and all transformation parameters are taken into account, a sparse linear equation system is built with $\mathbf{t}_{i,j}$ being the known parts of the equations:

$$\mathbf{A} \begin{bmatrix} \mathbf{p}_1 \\ \dots \\ \mathbf{p}_N \end{bmatrix} = \begin{bmatrix} \mathbf{t}_{1,2} \\ \dots \\ \mathbf{t}_{N,N-1} \end{bmatrix} \rightarrow \mathbf{A}\mathbf{p} = \mathbf{t}. \quad (2)$$

Since each image in a 4-connected neighborhood has two or more neighbors, this system is overdetermined. Such a system can be solved in a least square sense. To make the least square approach more robust we weight each equation with the peak correlation value of the transformation. This results in a diagonal weighting matrix $\mathbf{W}$ with the corresponding weighted least square problem:

$$\underset{\mathbf{p}}{\operatorname{argmin}}(\|\mathbf{W}(\mathbf{A}\mathbf{p} - \mathbf{t})\|_2). \quad (3)$$

Transforms that exhibit a correlation value of smaller than 0.15 are weighted with 0. Thus unreliable transforms are not taken into account. The threshold of 0.15 was empirically determined.

B. Analysis of positioning accuracy

Positioning accuracy of the microscope system is not only subject to the mechanical and controller accuracy of the stage but also subject to the accuracy of the calibration used. For example there might be direction dependent offsets because of miscalibration or rounding errors. Since we scan the slides in a meandering way, we have three different directions (left to right, right to left and top to bottom) that have to be analyzed separately. Since the stage is always moved for the same distance for each of the three mentioned directions the calibration dependent offset should be constant in the respective direction.

Our analysis is based on the error offset $\mathbf{t}_{\text{off}}$ between the transform parameters projected by moving the stage $\mathbf{t}_{\text{proj}}$ in the specific direction and the acquired transform parameters $\mathbf{t}$:

$$\mathbf{t}_{\text{off}} = \mathbf{t}_{\text{proj}} - \mathbf{t}. \quad (4)$$

To get a measurement of the calibration dependent offset, the mean in x- and y- direction of $\mathbf{t}_{\text{off}}$ could be calculated for the three scanning directions. While the inversely transformed normalized cross power spectrum is a very reliable estimator, in real-world applications misregistrations (outliers) happen. An outlier could be given a far too high weight using the mean. Thus, to make the estimation more robust we calculate the median in x-direction $\widetilde{\mu}_{\text{x}-\text{off}}$ and in y-direction $\widetilde{\mu}_{\text{y}-\text{off}}$ as an estimator for the calibration dependent offset in each of the three directions. The median

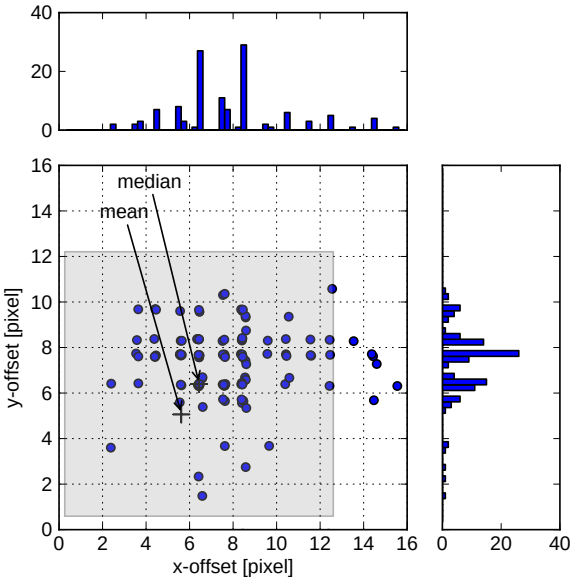

Fig. 2. Scatter plot including histograms of the calculated offsets between the projected stage translation and the measured stage translation according to Eq. 4. This plot is the result of a scan of 170 FoV when scanning left to right. The gray rectangle visualizes the bound constraints with ± 3 times the median absolute deviation with respect to the median in x- and y-direction.

is calculated by ordering a list of values from small to high and taking the middle one. The scatter plot with histograms shown in Fig. 2 visualizes the error offset (compare Eq. 4) of a typical scan when moving the stage from left to right. Additionally the mean and median as well as the bound constraint is marked. Clearly, the median gives a better estimate of the calibration dependent offset than the mean. Since the distribution in x- and y-direction is not Gaussian, the mean is further away from the distribution center than the median.

The mechanical and controller accuracy of the stage should then result in offsets that vary around the median. As an estimate of this we use the median absolute deviation in x-direction $\widetilde{\sigma}_{\mathrm{x-off}}$ and in y-direction $\widetilde{\sigma}_{\mathrm{y-off}}$. For simplicity in the remainder of the document the vector consisting of $\widetilde{\mu}_{\mathrm{x-off}}$ and $\widetilde{\mu}_{\mathrm{y-off}}$ will be denoted with $\widetilde{\mu}_{\mathrm{off}}$ and the vector consisting of the two median absolute deviation values with $\widetilde{\sigma}_{\mathrm{off}}$. These values can be used to specify upper and lower bounds for the variation of the possible position of the images. However empirically determined we got better result when using 3-times the absolute median deviation as boundary constraint. The schematic in Fig. 3 visualizes these constraints for 3×3 FoV.

Assuming that the images I_1 to I_N are in the successive order of the scan we get the following upper and lower constraints:

$$\mathbf{p}_{i+1} - \mathbf{p}_i \leq \mathbf{t}_{\mathrm{proj}_{i,i+1}} + \widetilde{\mu}_{\mathrm{off}} + 3 * \widetilde{\sigma}_{\mathrm{off}}, \; i \in [1, N-1] \quad (5)$$

$$\mathbf{p}_i - \mathbf{p}_{i+1} \leq -\mathbf{t}_{\mathrm{proj}_{i,i+1}} - \widetilde{\mu}_{\mathrm{off}} + 3 * \widetilde{\sigma}_{\mathrm{off}}, \; i \in [1, N-1] \quad (6)$$

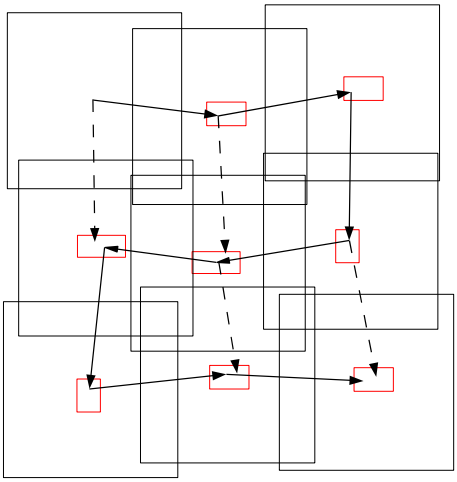

Fig. 3. Schematic of a scan of 3×3 FoV. The arrows mark the transformations acquired by the normalized cross power spectrum whereby the continuous arrows additionally show the order of the consecutive meandering scan performed by the stage. The red rectangles visualize the bounds in which each FoV can be relocated with respect to its direct predecessor in scan order. Note the three different sizes of the red rectangles marking the three different rectangular bounds for right to left, left to right and top to bottom scan order.

where $\widetilde{\mu}_{\mathrm{off}}$ and $\widetilde{\sigma}_{\mathrm{off}}$ are dependent on the direction of the scan as mentioned before. In matrix notation this leads to the non-equality constraint:

$$\mathbf{C}\mathbf{p} \leq \mathbf{b}. \quad (7)$$

C. Problem formulation

Resolving the weighted least squares equation system Eq. 3 and taking the constraints derived in Sec. IV-B into account, yields the following optimization problem:

$$\underset{\mathbf{p}}{\operatorname{argmin}}(\mathbf{t}^T\mathbf{W}^2\mathbf{t} - 2\mathbf{t}^T\mathbf{W}^2\mathbf{A}\mathbf{p} + \mathbf{p}^T\mathbf{A}^T\mathbf{W}^2\mathbf{A}\mathbf{p}) \quad (8)$$

$$\text{subject to}$$

$$\mathbf{C}\mathbf{p} - \mathbf{b} \leq 0.$$

A convex optimization problem with a quadratic function and non equality constraints is a quadratic program. Quadratic programs can be solved using the *Karush-Kuhn-Tucker* (KKT) theorem. The KKT theorem is basically an extension of the Lagrangian multipliers whereby the inequality constraints are either active or inactive. Active means that an inequality constraint really constraints the solution and thus is of Lagrangian type. While an inactive constraint is a constraint that is not constraining the solution and thereby not affecting the solution.

V. Evaluation

Stitching algorithms are typically only visually evaluated. Especially in microscopy an objective evaluation is a difficult task, since there is no ground truth available, that the stitched image can be compared against. In previous work, we therefore presented a method that is based on the generation

of cervical synthetic virtual slides to get a ground truth about the positioning accuracy of the stitching algorithm [8]. For the purpose of generating such a synthetic slide, on several real-world slides the distribution of the cells is analyzed and the average background color is measured. Subsequently, a scene is generated with the average background color matching the measured one. On this scene images of cervical cells and cervical cell clusters are distributed according to the measured real-world distribution. This scene is then cut in 1000×1000 pixel^2 FoV that each have roughly a 20% overlap to the adjacent images. To imitate the positioning accuracy of the stage, the cutting positions randomly vary around the projected cut. Each field is separately corrupted by additive white Gaussian noise. The fields can then be stitched using a mosaicing algorithm and the resulting FoV positions of the FoV can be compared against the actual known cut positions.

For this work we extended this approach to better match the real circumstances in microscopy. Thus we do not only let the cut position vary around the projected cut, but we also introduce additional offsets that are based on the measured median offsets for the three scanning directions of a real slide as introduced in Sec. IV-B. Additionally, since we want to prove that the algorithm is specifically suitable for slides with areas of low information content, we make sure that randomly with a probability of 20% the overlap areas between adjacent FoV are completely void of information content. Further, each FoV is shaded to simulate the brightness distribution present in microscopy. For the purpose of shading, an image of a area on a slide with no information content has been taken, as white reference image. The shading has been done by inversing the two-point calibration scheme using an empty black reference image, as for example defined by *Jähne* [12]. The size of the synthesized slides used for evaluation has been extended to 20×30 FoV. An example of such a synthetic slide is shown in Fig. 4.

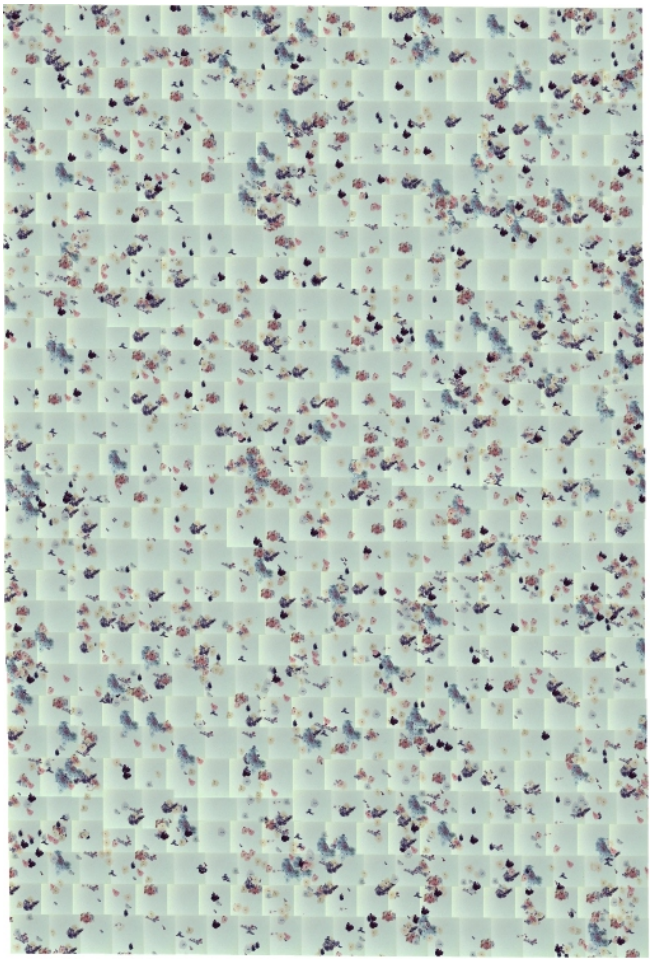

Fig. 4. An example of a 20×30 synthetic slide stitched with the presented method. The repetitive use of the same cells can be clearly observed as well as the shading that has been applied.

A. Evaluation on synthetic slides

150 synthetic slides each with 20×30 FoV have been generated. These slides were stitched using the presented algorithm. For comparison they were also evaluated using the weighted least squares optimization previously presented by us [8]. Additionally they were evaluated using standard least square optimization as introduce by [4] and using naive consecutive stitching without optimization. For each field of view the error metric is the relative Euclidean distance between the reference translational vector to every neighboring field of view and the translational vector that results from the different stitching schemes.

Tab. I reproduces the results obtained by the evaluation and clearly shows that the presented method yields the best results. At first glance the rather high mean error 1.82 pixel does not seem to be a very promising result. However, one has to be aware that these results also include FoV with empty overlap areas that cannot be exactly placed. Thus the median error of 0.820 pixel gives a better estimate of the positioning accuracy. Considering this it is clear that the vast majority of all FoV could be accurately placed. The weighted least squares optimization scheme yields good results with a median positioning error of 0.822 pixel. However considering that the mean and standard deviation is much higher compared to the proposed scheme, the stitched results are not as consistent. These results clearly show that constraining the solution yields a more consistent mosaic. The worse results obtained by the optimization using standard least squares optimization stem from the characteristics of the method. Standard least squares optimization just distributes the error evenly over all equations and does not distinguish between good and bad fits. The naive consecutive alignment without optimization show the expected bad results.

B. Visual Evaluation

The presented algorithm was furthermore tested visually on several real-world examples. Slides from histology, cervical cells and blood smears were scanned and then stitched. Fig. 5 exemplary shows a histologic slide of artificially grown human skin tissue stitched with the presented method. By visual inspection almost no offsets between neighboring

TABLE I

POSITIONING ERROR RESULTS OBTAINED BY EVALUATING 150 SYNTHETIC SLIDES OF SIZE $20 * 30$ FOV AND A PROBABILITY OF AN EMPTY OVERLAP AREA OF 20%. THE ERROR IS GIVEN AS MEAN μ_e, STANDARD DEVIATION σ_e, MEDIAN $\widetilde{\mu}_e$, MINIMUM min_e[pixel] AND MAXIMUM max_e OF THE EUCLIDEAN DISTANCE BETWEEN THE SUPPOSED TRANSLATIONAL VECTOR TO THE NEIGHBORING FIELDS OF VIEW AND THE TRANSLATIONAL VECTOR CALCULATED BY STITCHING.

Algorithm	$\mu_e \pm \sigma_e$ [pixel]	$\widetilde{\mu}_e$ [pixel]	$\min_e[pixel]$	$\max_e$ [pixel]
Consecutive alignment	208.679 ± 279.442	104.766	0.003	2620.28
Least squares optimized stitching	60.976 ± 48.521	47.789	0.100	424.102
Weighted least squares optimized stitching	4.111 ± 12.523	0.822	0.002	307.827
Quadratic programming based optimization	1.820 ± 2.774	0.820	0.002	71.881

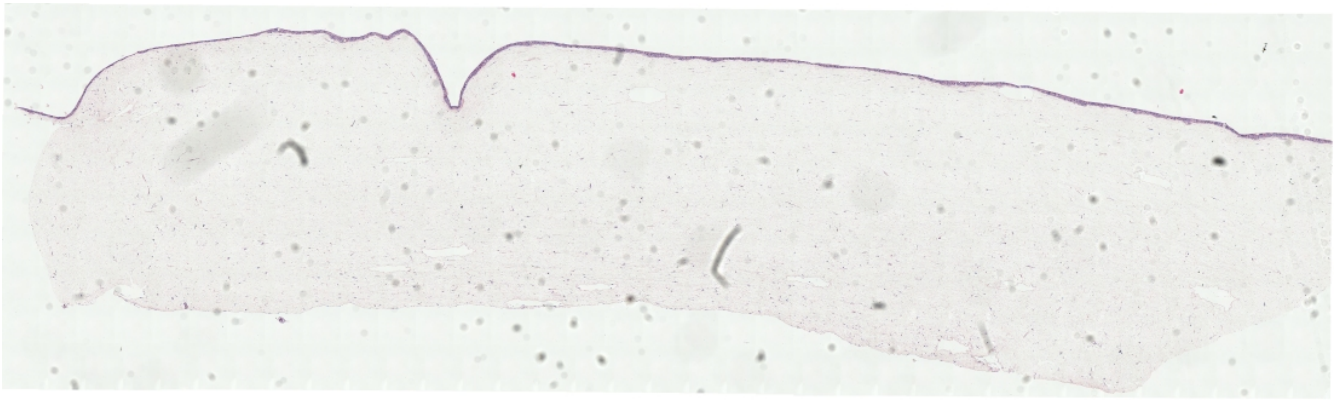

Fig. 5. An example of a histologic specimen of artificially grown human skin tissue. 35×10 FoV were scanned using a $20-$fold objective. The FoV were mosaiced using the proposed method. (Skin equivalent courtesy of Fraunhofer IGB, Department Cell and Tissue Engineering.)

FoV could be distinguished. This shows that the proposed synthetic evaluation can give a ground truth about the positioning accuracy of the stitching schemes under worst case assumptions. But in real-world applications neither the shading is as extreme nor are there usually so many empty overlap areas. Thus, one should not take the values as presented in Tab. I as absolute but rather as a means of ground truth comparison of different stitching schemes.

VI. CONCLUSION

We presented an extension of our algorithm for automatic stitching of microscopy images. We treat stitching as a parameter optimization problem which we solve globally for all images in parallel. Non-equality constraints make it necessary to apply an optimization technique that can handle such constraints. Using the *Karush-Kuhn-Tucker* theorem we use quadratic programming to solve the system of equations.

As in our previous work, we did our best to provide quantitative evaluations under realistic conditions. We extended the method that uses synthetic images to provide accurate ground truth. We also used real-world images and evaluated the results. The results show visually and quantitatively that our mosaicing algorithm provides highly accurate results.

ACKNOWLEDGMENTS

This work was partly supported by the International Max-Planck Research School for Optics and Imaging.

REFERENCES

[1] F. Leong and J. McGee, "Automated complete slide digitization: a medium for simultaneous viewing by multiple pathologists," *The Journal of Pathology*, vol. 195, no. 4, pp. 508–514, 2001.

[2] K. Saeger, K. Schlüns, T. Schrader, and P. Hufnagl, "The virtual microscope for routine pathology based on a pacs system for 6 gb images," in *International Congress Series*, vol. 1256. Elsevier, 2003, pp. 299–304.

[3] R. Szeliski, *Image Alignment and Stitching: A Tutorial*. Now Publishers Inc, 2006.

[4] J. Davis, "Mosaics of scenes with moving objects," in *Computer Vision and Pattern Recognition, 1998. Proceedings. 1998 IEEE Computer Society Conference on*, 23-25 June 1998, pp. 354–360.

[5] E.-Y. Kang, I. Cohen, and G. Medioni, "A graph-based global registration for 2d mosaics," in *Proc. 15th International Conference on Pattern Recognition*, I. Cohen, Ed., vol. 1, 2000, pp. 257–260 vol.1.

[6] C. Sun, R. Beare, V. Hilsenstein, and P. Jackway, "Mosaicing of microscope images," in *Proc. Digital Image Computing: Technqiues and Applications DICTA ' 05*, R. Beare, Ed., 2005, pp. 343–348.

[7] B. Appleton, A. Bradley, and M. Wildermoth, "Towards optimal image stitching for virtual microscopy," in *Proc. Digital Image Computing: Technqiues and Applications DICTA ' 05*, A. Bradley, Ed., 2005, pp. 299–306.

[8] D. Steckhan, T. Bergen, T. Wittenberg, and S. Rupp, "Efficient large scale image stitching for virtual microscopy," in *Proceedings of the 30th Annual International Conference of the IEEE EMBS*, Aug. 2008, pp. 4019–4023.

[9] D. Steckhan and T. Wittenberg, "Optimized graph-based mosaicking for virtual microscopy," in *Medical Imaging 2009: Image Processing*, vol. 7259, Jan. 2009.

[10] H. Foroosh, J. Zerubia, and M. Berthod, "Extension of phase correlation to subpixel registration," *IEEE Trans. Image Processing*, vol. 11, no. 3, pp. 188–200, 2002.

[11] J. Proakis and M. Salehi, *Digital Communications*. McGraw-Hill New York, 1995.

[12] B. Jähne, *Digital image processing: concepts, algorithms and scientific applications*. Springer-Verlag London, UK, 1991.

[13] D. Wald, M. Reeff, G. Szkely, P. Cattin, and D. Paulus, "Fließende Überblendung von Endoskopiebildern für die Erstellung eines Mosaiks," in *Bildverarbeitung für die Medizin 2005*, H. P. Meinzer, H. Handels, A. Horsch, and T. Tolxdorff, Eds. Springer, Berlin, Heidelberg, New York, 3 2005, pp. 287–291. [Online]. Available: ftp://ftp.vision.ee.ethz.ch/publications/proceedings/eth_biwi_00339.pdf